

SUPPORTING INFORMATION

Altermagnetic surface states: towards the observation and utilization of altermagnetism in thin films, interfaces and topological materials

Raghottam M Sattigeri ^{1,*} Giuseppe Cuono ^{1,†} and Carmine Autieri ^{1,‡}

¹*International Research Centre Magtop, Institute of Physics,
Polish Academy of Sciences, Aleja Lotników 32/46, PL-02668 Warsaw, Poland*

(Dated: September 8, 2023)

I. COMPUTATIONAL DETAILS

We performed density functional theory-based *first-principles* calculations as implemented in Quantum ESPRESSO.¹ We performed the calculations without spin-orbit coupling effects. The antiferromagnetic ground state was obtained using ultra-soft pseudopotentials under generalized gradient approximation with Perdew–Burke–Ernzerhof type of exchange-correlation functional.^{2,3} The kinetic energy cut-off of 65 Ry and charge density cut-off of 780 Ry were used with a Monkhorst-Pack grid (k -mesh) of $12 \times 12 \times 8$.⁴ High electronic self-consistency convergence criteria of at least 10^{-10} were followed in all the calculations. The antiferromagnetic ground state of RuO₂ was obtained by implementing Hubbard U with GGA for Ru atoms with $U = 2$ eV and $J_H = 0.15U$. After these calculations, we performed wannierization for all the systems using Wannier90 code.⁵ In the wannierization process, the disentanglement procedure was followed with convergence criteria of 10^{-11} . For LaMnO₃ the projectors used were for Mn sites d_{z^2} , d_{xy} ; for MnTe the projectors were for Mn sites d and for Te sites p ; and for RuO₂ the projectors were for Ru sites d_{xy} , d_{xz} , d_{yz} and for O sites p . The exact tight-binding Hamiltonian generated from wannierization was then used to calculate the altermagnetic surface states using semi-infinite Green's function approach implemented in WannierTools code.⁶

We have tested the slab calculations for different slab thicknesses of 5, 10, 15 and 20 repetitions we do not find any appreciable difference in the altermagnetic spin-splitting except for the number of bands as evident from Fig. S1.

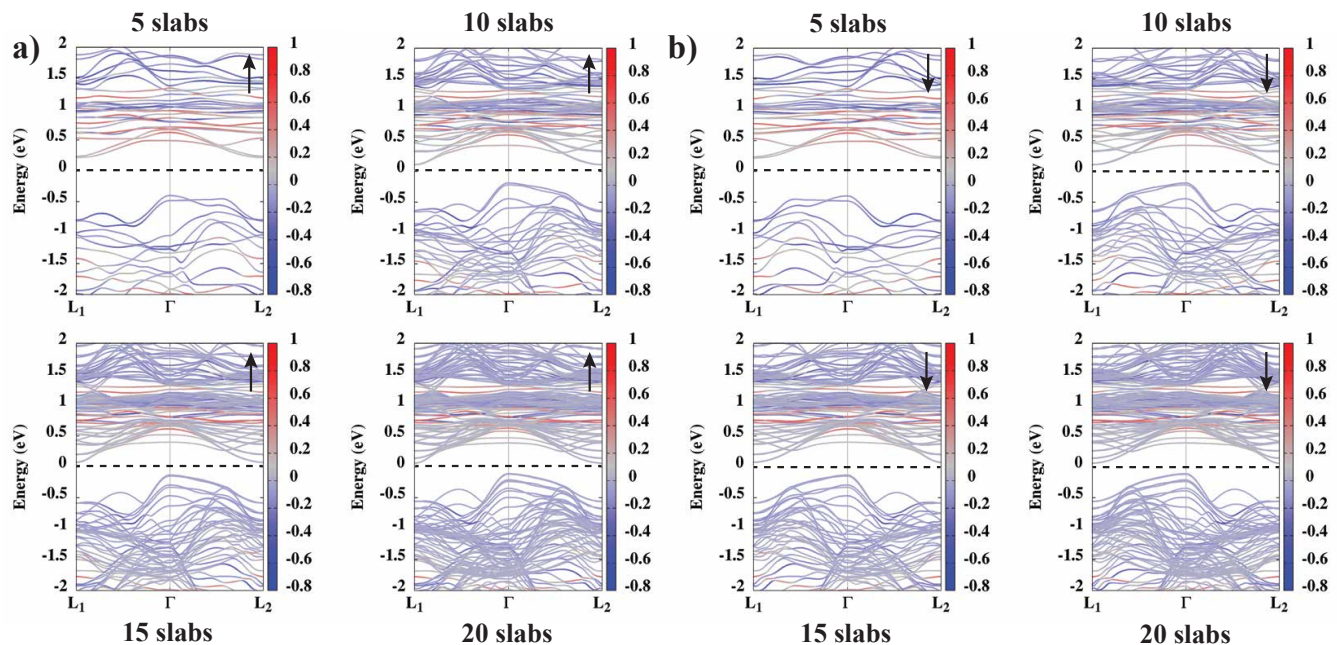


FIG. S1. Slab band structures for (a) spin-up channel and (b) spin-down channel of MnTe for different slab thickness.

II. NOTATIONS AND STRUCTURAL DETAILS

Within this paper, (xyz) is the notation to describe the surface plane, while $[xyz]$ is the notation for the direction orthogonal to the surface plane. We report the crystal symmetries and the structural details of the investigated compounds for a complete understanding of the surface orientations described in the main text. The crystal structures are presented in Fig. S2. The Bravais lattice vectors for space group no. 62 are $\mathbf{a}_1=(a,0,0)$, $\mathbf{a}_2=(0,b,0)$ and $\mathbf{a}_3=(0,0,c)$ while the reciprocal lattice vectors are $\mathbf{b}_1=(\frac{2\pi}{a},0,0)$, $\mathbf{b}_2=(0,\frac{2\pi}{b},0)$ and $\mathbf{b}_3=(0,0,\frac{2\pi}{c})$. The Bravais lattice vectors for space group no. 136 are $\mathbf{a}_1=(a,0,0)$, $\mathbf{a}_2=(0,a,0)$ and $\mathbf{a}_3=(0,0,c)$ while the reciprocal lattice vectors are $\mathbf{b}_1=(\frac{2\pi}{a},0,0)$, $\mathbf{b}_2=(0,\frac{2\pi}{a},0)$ and $\mathbf{b}_3=(0,0,\frac{2\pi}{c})$. The Bravais lattice vectors for space group no. 194 are $\mathbf{a}_1=(\frac{a}{2},\frac{a\sqrt{3}}{2},0)$, $\mathbf{a}_2=(\frac{a}{2},-\frac{a\sqrt{3}}{2},0)$ and $\mathbf{a}_3=(0,0,c)$. The reciprocal lattice vectors are $\mathbf{b}_1=(\frac{2\pi}{a},\frac{2\pi}{a\sqrt{3}},0)$, $\mathbf{b}_2=(\frac{2\pi}{a},-\frac{2\pi}{a\sqrt{3}},0)$ and $\mathbf{b}_3=(0,0,\frac{2\pi}{c})$. The $[110]$ k -space direction is parallel to the vector $\mathbf{b}_1+\mathbf{b}_2=(\frac{4\pi}{a},0,0)$.

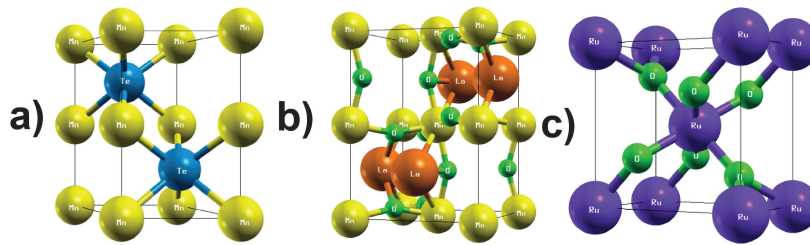


FIG. S2. Crystal structures for a) hexagonal MnTe (yellow balls are Mn and blue balls are Te), b) orthorhombic LaMnO₃ (orange balls are La, yellow balls are Mn, and green balls are O) and c) tetragonal RuO₂ (purple balls are Ru and green balls are O) obtained from the materials project repository.⁷

The lattice parameters for the three systems under consideration were obtained from the materials project repository⁷. The optimized lattice parameters used for MnTe were $a=4.107$ Å and $c=6.467$ Å. For LaMnO₃ we used the Pbnm setting⁸ with $a=5.585$ Å, $b=5.871$ Å and $c=7.777$ Å while for RuO₂ we performed the calculations with $a=b=4.482$ Å and $c=3.111$ Å. MnTe and RuO₂ have two magnetic atoms in the unit cells, therefore only one antiferromagnetic configuration is possible. LaMnO₃ is an orthorhombic perovskite with the four Mn magnetic atoms in the 4b Wyckoff positions, the A-type magnetic order consists of the 2 Mn atoms at $z=0$ with spin-up and 2 Mn atoms at the reduced coordinates $z=0.5$ with spin-down⁹.

III. SURFACE UNCOMPENSATED MAGNETISM ON (001) SURFACE OF MNTE

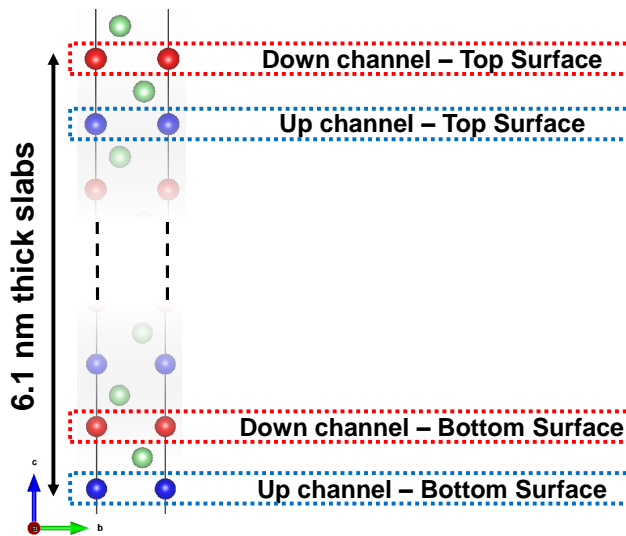


FIG. S3. Asymmetric and stoichiometric slab of MnTe with (001) surface orientation. Red and blue balls represent the spin-down and spin-up Mn atoms, while green balls represent the Te atoms. The surfaces are inequivalent, the top surface ends with oxygen while the bottom surface ends with Mn.

The spin-up channel and spin-down channel surface states of the (001) surface orientation of MnTe slightly differ due to surface uncompensated magnetism. Indeed, the (001) slab is asymmetric as we can see in Fig. S3. The two terminations of the slab (top and bottom) are inequivalent, therefore, the spin-up and spin-down channels are inequivalent. The surface band structures for the spin-up and spin-down channels and for top and bottom surfaces are reported in Fig. S4. We can observe minor differences among all cases. In the case of DFT simulations with a symmetric slab (that however will not preserve the stoichiometry), we would recover the symmetries observed in the RuO₂ case.

The same effect of the surface uncompensated magnetism is present on the (001) surface of LaMnO₃, however, the alternating spin-splitting in LaMnO₃ is one order of magnitude smaller than MnTe, therefore, this uncompensated

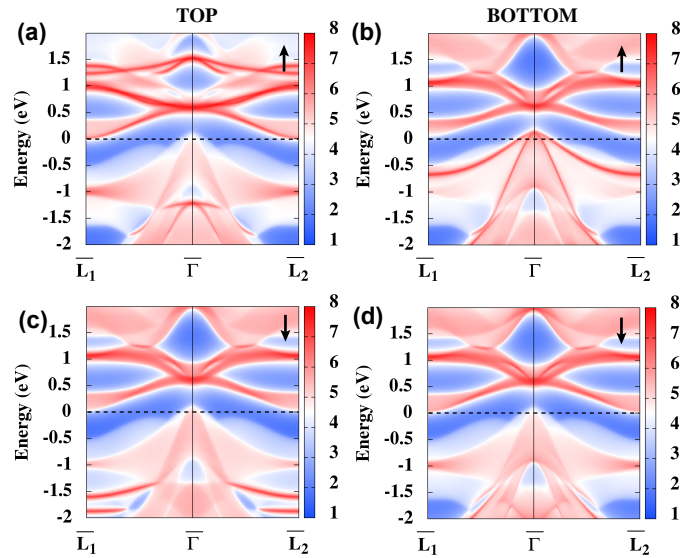


FIG. S4. Electronic surface states of MnTe along the k -path $\bar{L}_1\text{-}\bar{\Gamma}\text{-}\bar{L}_2$ for the (a,b) spin-up channel projected on the (001) surface orientation for the (a) top and (b) bottom surfaces, respectively. (c,d) The same for the spin-down channel. Due to the surface uncompensated magnetism, all these surface band structures are different. The Fermi level is set to zero. In the surface band structure, the red color means large spectral weight while the blue color means zero spectral weight.

magnetism effect is not appreciable in LaMnO_3 .

IV. $(\bar{1}\bar{1}0)$ SURFACE: THE NON-ALTERMAGNETIC SURFACE OF MNTE

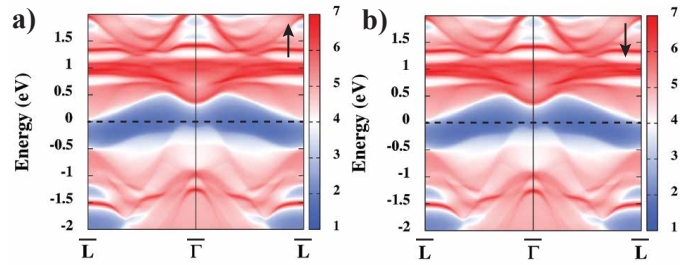


FIG. S5. Non-altermagnetic surface states of MnTe shows that the surface states for spin-up channel and spin-down channel are indistinguishable.

* rsattigeri@magtop.ifpan.edu.pl

† gcuono@magtop.ifpan.edu.pl

‡ autieri@magtop.ifpan.edu.pl

¹ Paolo Giannozzi, Stefano Baroni, Nicola Bonini, Matteo Calandra, Roberto Car, Carlo Cavazzoni, Davide Ceresoli, Guido L Chiarotti, Matteo Cococcioni, Ismaila Dabo, *et al.*, “Quantum espresso: a modular and open-source software project for quantum simulations of materials,” *Journal of physics: Condensed matter* **21**, 395502 (2009).

² Gianluca Prandini, Antimo Marrazzo, Ivano E Castelli, Nicolas Mounet, and Nicola Marzari, “Precision and efficiency in solid-state pseudopotential calculations,” *npj Computational Materials* **4**, 72 (2018).

³ John P Perdew, Kieron Burke, and Matthias Ernzerhof, “Generalized gradient approximation made simple,” *Physical review letters* **77**, 3865 (1996).

⁴ Hendrik J Monkhorst and James D Pack, “Special points for brillouin-zone integrations,” *Physical review B* **13**, 5188 (1976).

- ⁵ Arash A Mostofi, Jonathan R Yates, Giovanni Pizzi, Young-Su Lee, Ivo Souza, David Vanderbilt, and Nicola Marzari, “An updated version of wannier90: A tool for obtaining maximally-localised wannier functions,” *Computer Physics Communications* **185**, 2309–2310 (2014).
- ⁶ QuanSheng Wu, ShengNan Zhang, Hai-Feng Song, Matthias Troyer, and Alexey A Soluyanov, “Wanniertools: An open-source software package for novel topological materials,” *Computer Physics Communications* **224**, 405–416 (2018).
- ⁷ Anubhav Jain, Shyue Ping Ong, Geoffroy Hautier, Wei Chen, William Davidson Richards, Stephen Dacek, Shreyas Cholia, Dan Gunter, David Skinner, Gerbrand Ceder, *et al.*, “Commentary: The materials project: A materials genome approach to accelerating materials innovation,” *APL materials* **1**, 011002 (2013).
- ⁸ C. Autieri, M. Cuoco, G. Cuono, S. Picozzi, and C. Noce, “Orbital order and ferromagnetism in lamn1–xgaxo3,” *Physica B: Condensed Matter* **648**, 414407 (2023).
- ⁹ Giuseppe Cuono, Raghottam M. Sattigeri, Jan Skolimowski, and Carmine Autieri, “Orbital-selective altermagnetism and correlation-enhanced spin-splitting in strongly-correlated transition metal oxides,” *Journal of Magnetism and Magnetic Materials* **586**, 171163 (2023).